

Synthesis of Novel Chitosan Derivatives for Micellar Solubilization of Cyclosporine A

XIAOLEI CHEN, SONG DING, GUOWEI QU AND CAN ZHANG*

Centre for Drug Discovery

China Pharmaceutical University, Nanjing 210009, PR China

ABSTRACT: In this study, the solubilization of poor water-soluble drugs using *N*-acyl, *O*-acyl-*N*-trimethyl chitosan chloride (ATMC) micelles as a carrier system was investigated. Three series of ATMCs were synthesized by *N*-trimethyl chitosan chloride (TMC) with substitutions of 21.3, 44.8, and 45.2% as start material grafting five different long-chain saturated fatty acids (C₁₀–C₁₈), and characterized by ¹H-NMR, ¹³C-NMR, and FT-IR spectra, respectively. The degree of long-chain acyl group of ATMC was ~8.1%. These ATMC micelles self-assemble and were used to encapsulate the poorly soluble drug, Cyclosporine A. These assemblies were prepared by a dialysis, wherein the drug loading capacity of the ATMC micelles ranged from 9.6% to 17.1% and encapsulation capacity ranged from 35.8% to 69.8%, with the mean micellar particle size of 288 nm. The critical micellar concentrations of the 70,000 Mw ATMC2 were 0.028–0.038 mg/mL. Nanoscale near-spherical ATMC micelles were observed by transmission electron microscopy. Additionally, the chitosan derivatives with a high methylation degree, medium-sized long-chain acyl groups (C₁₄) and large molecular weight had the most effective capacity for loading Cyclosporine A. These ATMC micelles are being investigated as carriers to improve oral administration absorption of poorly permeable drugs.

KEY WORDS: drug delivery, chitosan, trimethyl chitosan, saturated fatty acid, absorption enhancer, micelle, Cyclosporine A, solubilization of insoluble drugs.

INTRODUCTION

The problem of poor water-soluble drugs is that it restricts their clinical application and effective strategies to overcome this

*Author to whom correspondence should be addressed. E-mail: zhangcan@cpu.edu.cn

limitation are required. Recently, the polymeric micelles, formed by amphiphilic copolymers, are being investigated to conquer this problem by encapsulating the poorly soluble agents [1]. In aqueous media, amphiphilic copolymers spontaneously assemble to form a micellar structure above their critical micelle concentration (CMC) with hydrophilic shell and hydrophobic core. This allows poorly soluble drugs to be encapsulated within the hydrophobic inner core [2]. In a sense, micelles can sufficiently enhance the water solubility and bioavailability of various poorly soluble drugs. The immunosuppressant drug, Cyclosporine A (CyA) is a hydrophobic drug that has low bioavailability after oral administration due to its poor solubility.

Chitosan, a natural aminopolysaccharide obtained by hydrolysis of chitin, is a pharmaceutical excipient for drug delivery because it has favorable biological properties, such as biocompatibility, biodegradability, positive charge, nontoxicity, and bioadhesivity [3–5]. However, in spite of many reported successes, the major drawback of chitosan is its poor solubility at physiological pH, whereas it is soluble only in acidic environments with pH values lower than 6.0; this limits its application in the pharmaceutical field. Several efforts have been made to chemically modify chitosan and numerous derivatives of chitosan have been synthesized to meet the requirements for drug delivery systems [6–9], such as peroral peptide delivery systems [10–12] because of their permeation enhancing effect, enzyme inhibitory capabilities, and mucoadhesive properties.

N-Trimethyl chitosan chloride (TMC), a partially quaternized chitosan derivative, is soluble in the entire pH range. It has been used as an absorption enhancer for peptide drugs by opening the tight junctions between epithelial cells, thereby facilitating the paracellular transport of hydrophilic compounds and peptide drugs [13,14]. However, TMC is a hydrophilic polymer which lacks any hydrophobic segments, so that it does not form micelles for solubilization in aqueous media. Therefore, hydrophobically modified TMC were constructed by chemically conjugating the hydrophobic segments to the hydrophilic TMC backbone.

In previous work, we reported that the chitosan-based amphiphilic polymer *N*-octyl-*O*-sulfate chitosan was a safe polymeric material to load paclitaxel which improved drug solubility, prolonged drug circulation time, and reduced drug toxicity [15,16]. Herein, we report a series of novel TMC-based amphiphilic polymer, *N*-acyl, *O*-acyl-*N*-trimethyl chitosan chloride (ATMC), by coupling long-chain saturated fatty acids, such as decanoic acid, lauric acid, myristic acid, palmitic acid, and stearic acid as hydrophobic segments since they are widely available

and are potentially safe permeation enhancers for peptides and nonpeptides [17]. Several chitosan derivatives were synthesized and their structures were fully confirmed by $^1\text{H-NMR}$, $^{13}\text{C-NMR}$, and FT-IR spectra. The AMTC micelles, composed of a hydrophilic shell of TMC and hydrophobic cores of the long-chain acyl groups, through a dialysis method. The hydrophobic drug, CyA, was successfully loaded into the AMTC micelles; the loading capacity (LC), encapsulation capacity (EC), and micelle particle size were determined. Based on the experimental results, the relationship between the structural properties of chitosan derivatives (such as molecular weight, methylation degree and different hydrophobic segments) and micellar drug-loading were determined.

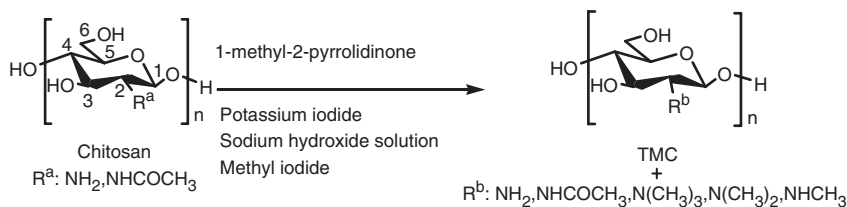
MATERIALS AND METHODS

Materials

Two different chitosan samples were provided by the Nantong Suanglin Biochemical Co. Ltd (China) with deacetylation degrees of 92% (DA = 8%) and viscosity average Mw of 70,000 and 29,000. Pyrene was purchased from Fluka Company (>99%). Long-chain saturated fatty acids were from Sinopharm Chemical Reagent Co., Ltd (China). Cyclosporine A (CyA) was supplied by IVAX Pharmaceuticals s.r.o. (>99%) Czechoslovakia). All commercially available solvents and reagents were used without further purification.

Synthesis of *N*-trimethyl Chitosan Chloride

TMC polymers were synthesized by reductive methylation of chitosan by the chemical reaction between chitosan and iodomethane in the presence of sodium hydroxide according to the method described by Sieval [9]. The reaction depicted in Scheme 1 was repeated several times with the product obtained from previous step to obtain TMC polymers



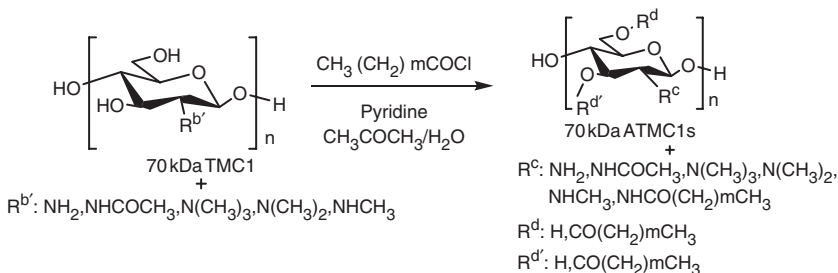
Scheme 1. Synthesis of TMC preparation.

with different degrees of methylation. So *N*-trimethyl chitosan chloride with low methylation (70,000 TMC1) was gained by a one-step synthesis of methylation while *N*-trimethyl chitosan chloride with high methylation (70,000 TMC2 and 29,000 TMC2) were prepared by a two-step synthesis of methylation.

Synthesis of *N*-acyl, *O*-acyl-*N*-trimethyl Chitosan Chloride

A 100 mL three-neck flask, equipped with a reflux condenser and a dropping funnel, was loaded with decanoic acid (3.7 g, 22 mmol) and heated at 84°C with an oil bath to melt the acid [18]. A mixture of thionyl chloride (SOCl₂, 7.85 g, 66 mmol) and dimethyl formamide (DMF, 0.5 mmol) was added slowly at 84°C within 30 min. After 5 h the product was recovered by removing the excess SOCl₂ under vacuum conditions. The average product yield was ~95%.

The synthetic route leading to 70,000 ATMC1s from 70,000 TMC1 (Scheme 2) was as follows: 70,000 TMC1 (1.0 g, 6 mmol) was dissolved in 30 mL of the aqueous solution with trifluoroacetic acid (0.1 mL, 1.3 mmol) [19] and the acetone (80 mL) was added under intense stirring. Pyridine (3.9 g, 44 mmol) dissolved in acetone (40 mL) was first added dropwise into the mixture and then a solution of decanoyl chloride (40 mmol) obtained by the above method in acetone (40 mL) was loaded later on. The reaction lasted for 12 h and then the mixture was poured into ice water, subsequently the suspension was filtered and the filter liquor was extracted by diethyl ether for 5 times, dialyzed by dialysis membranes (MWCO, 10,000) against distilled water for 3 d, and lyophilized further. Ultimately, 70,000 TMC1DG was obtained. 70,000 TMC1LG, 70,000 TMC1MG, 70,000 TMC1PG, and 70,000 TMC1SG were also gained by the same process of 70,000 TMC1 with lauric acid, myristic acid, palmitic acid, and stearic acid, respectively.



Scheme 2. Synthesis of *N*, *O*-acyl group-*N*-trimethyl chitosan chloride (70 kDa ATMC1s).

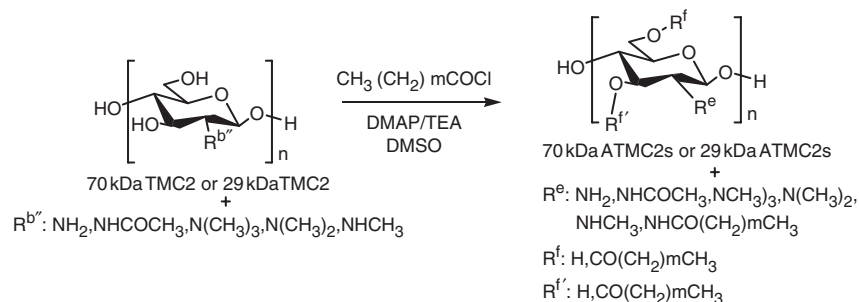
The synthetic route leading to 70,000 ATMC2s from 70,000 TMC2 (Scheme 3): 70,000 TMC2 (1.0 g, 6 mmol) was dispersed in 60 mL of dimethylsulfoxide (DMSO) with magnetic stirring for 2–3 h, then 4-dimethylaminopyridine (DMAP, 4 mmol) and triethylamine (TEA, 22 mmol) were added, respectively. Decanoyl chloride (22 mmol) was added dropwise into the mixture which was cooled in an ice-water bath [20]. After 0.5 h, the reaction mixture was allowed to come to ambient temperature with continual stirring for 12 h. The mixture was then poured into ice-water and the suspension was filtered, the filter liquor was extracted 5 times with diethyl ether, dialyzed by dialysis membranes (MWCO, 10,000) against distilled water for 3 d and freeze-dried. The 70,000 TMC2DG was obtained with 8.8% DS of decanoyl. Subsequently, 70,000 TMC2LG, 70,000 TMC2MG, 70,000 TMC2PG, and 70,000 TMC2SG were synthesized using the same procedure of 70,000 TMC2 with lauric acid, myristic acid, palmitic acid, and stearic acid, respectively.

The 29,000 TMC2DG, 29,000 TMC2LG, 29,000 TMC2MG, 29,000 TMC2PG, and 29,000 TMC2SG were also prepared using the same reaction of 29,000 TMC2 with decanoic acid, lauric acid, myristic acid, palmitic acid, and stearic acid, respectively.

Characterization of Chitosan Derivatives

$^1\text{H-NMR}$ and $^{13}\text{C-NMR}$ spectra were performed on a Bruker (AVACE) AV-300 spectrometer. The chitosan was dissolved in a mixed solvent of D_2O and CF_3COOD and the chitosan derivatives were dissolved in D_2O or a mixed solvent of D_2O and CF_3COOD .

FT-IR spectra were recorded on Fourier-transform infrared spectrometer (Nicolet 2000) in KBr discs.



Scheme 3. Synthesis of *N*-acyl, *O*-acyl group-*N*-trimethyl chitosan chloride (70 kDa ATMC2s and 29 kDa ATMC2s).

Measurement of the CMC

The CMC of the 70,000 ATMC2 was determined by using pyrene (Fluka, >99%) as a hydrophobic probe in fluorescence spectroscopy (Shimadzu RF-5301 PC, Japan) [21,22]. Briefly, pyrene in acetone was added to a series of 10 mL vials and the acetone was evaporated at room temperature, 5 mL of various concentrations of 70,000 ATMC2 solutions (2.5×10^{-4} – 1 mg/mL) were added to the vials (the final concentration of pyrene was controlled to 6×10^{-7} M). The vials were then sonicated for 30 min at ambient temperature. The sample solutions were heated at 65°C for 3 h to equilibrate the pyrene and the micelles and then left to cool overnight. Fluorescence excitation spectra were measured at the emission wavelength of 390 nm, and excitation wavelength was in the range of 300–360 nm, with excitation band width at 3 nm and emission band width at 5 nm. Based on the pyrene excitation spectra and red shift of the spectra with 70,000 ATMC2 concentrations increasing, the CMCs of the 70,000 ATMC2 were measured.

Preparation and Characterization of Polymeric Micelles of CyA

The ATMC polymeric micelles formed by self-assembling in a diluted aqueous solution. Poorly soluble drug CyA was loaded entrapped in the ATMC micelles through the following steps [23]: 10 mg ATMC in 4 mL distilled water were stirred ~ 2 h at room temperature for full dissolution; then 3 mg of CyA, dissolved in 200 μL of ethanol, was added dropwise into the aqueous ATMC solution with stirring, followed by dialysis against distilled water overnight by in dialysis membranes (MWCO, 10,000). The micellar solution was then centrifuged at 4000 rpm for 10 min and filtered through a 0.8 μm pore-sized microfiltration membrane to remove the residual CyA. The diameter and polydispersity (V) of the polymeric micelles were measured by Zetasizer 3000HS instrument (Malvern Instruments, Malvern, UK) with 633 nm He–Ne lasers at 25°C . The micellar solution was placed on a copper grid coated with framer film and transmission electron microscopy (TEM) analysis was performed using the micellar solution with a JEM-200CX (JEOL Ltd Japan).

Determination of CyA by HPLC Analysis

The amount of CyA encapsulated in the micelles was determined by HPLC (Agilent 1100, Agilent, Germany) using a DiamohsilTM C₁₈ column (250 \times 4.6 mm, 10 μm particle size) [24]. The mobile phase consisted of methanol: water: phosphoric acid (90:9.8:0.2, v: v: v) and the HPLC was

performed with a flow rate of 1.0 mL/min, with a column temperature at 55°C and a detection wavelength of 210 nm (Agilent 8453, UV detector, Agilent, Japan). The injected volume was 20 µL for all samples tested and the retention time of the CyA was 4.3 min. The drug LC and encapsulation efficiency (EE) of polymeric micelles of CyA:

$$\text{Loading capacity (LC)\%} = \left[\frac{C \times V}{(W_{\text{ATMC}})} \right] \times 100 \quad (1)$$

$$\text{Encapsulation efficiency (EE)\%} = \left[\frac{C \times V}{(W_{\text{CyA}})} \right] \times 100 \quad (2)$$

where C , V , W_{ATMC} , and W_{CyA} represented the CyA concentration of micelle solution, the volume of micelle solution, the weight of micelles after freeze-drying and the weight of CyA feeded, respectively.

RESULTS AND DISCUSSION

A series of *N*-trimethyl chitosan chloride (TMC) derivatives were prepared for evaluation for micelle formation and loading. The synthesis of TMC was completed by methylating chitosan with iodomethane in the presence of base as described in Scheme 1. The corresponding long-chain saturated fatty acids, decanoic acid, lauric acid, myristic acid, palmitic acid, and stearic acid were conjugated to the TMC backbone as hydrophobic segments to afford 15 ATMC derivatives. These were divided into three series 29,000 ATMC2s, 70,000 ATMC1s, and 70,000 ATMC2s. For each series of derivatives, a specific procedure for each reaction was adopted to obtain the polymer with similar degree of methylation and degree of acyl substitution. It was noted that due to the introduction of the long-chain acyl groups with the quaternary amino group on the chitosan backbone, that the inter-or intra-molecular hydrogen bonding of chitosan was disrupted and that the crystallinity was weakened as well as increasing the solubility of polymers in water [25]. All of the polymers obtained were purified by dialysis against water and freeze-dried. Structures were confirmed by $^1\text{H-NMR}$, $^{13}\text{C-NMR}$, and FT-IR analysis.

The degree of quaternization (DQ%) of TMC was determined according to the following Equation [26]:

$$\text{DQ\%} = \left[\frac{(\text{CH}_3)_3}{[\text{H}]} \right] \times \frac{1}{9} \times 100 \quad (3)$$

where $[(\text{CH}_3)_3]$ was the integral of the hydrogens of the trimethyl amino group at 3.3 ppm and $[\text{H}]$ was the integral of the hydrogen peaks between 4.7 and 5.7 ppm.

The $^1\text{H-NMR}$ spectrum of the 70,000 TMC1, obtained from the one-step methylation, resonance a peak at 3.3 ppm, for the $\text{N}^+(\text{CH}_3)_3$ protons [9], was used to calculate the DQ of 70,000 TMC1, which was 21.3%. Additionally, the DQ of the TMC polymers increased with the number of reaction steps used in the synthesis procedure. Taking into account the fact that the TMC polymers with various DQ display different physiochemical properties, the reaction of methylation with the TMC1 was repeated to a two-step methylated chitosan (TMC2) to synthesize the TMC polymers (70,000 TMC2 and 29,000 TMC2) with high DQ. The NMR signals at 3.4 ppm were attributed to $\text{N}^+(\text{CH}_3)_3$, DQ of 70,000 TMC2 and 29,000 TMC2 were 44.8% and 45.2%, respectively.

The successful conjugation of long-chain saturated fatty acids to the TMC backbones primarily was based on the $^1\text{H-NMR}$ analysis for both the TMC and ATMC. Compared with $^1\text{H-NMR}$ spectrum of the 29,000 TMC2, the $^1\text{H-NMR}$ spectra of the 29,000 ATMC2s in Figure 1 show new-emerged peaks at δ (ppm) 0.8–1.85 which were attributed to the $-\text{CH}_2$ and $-\text{CH}_3$ of the long-chain acyl substituents. However, a few differences

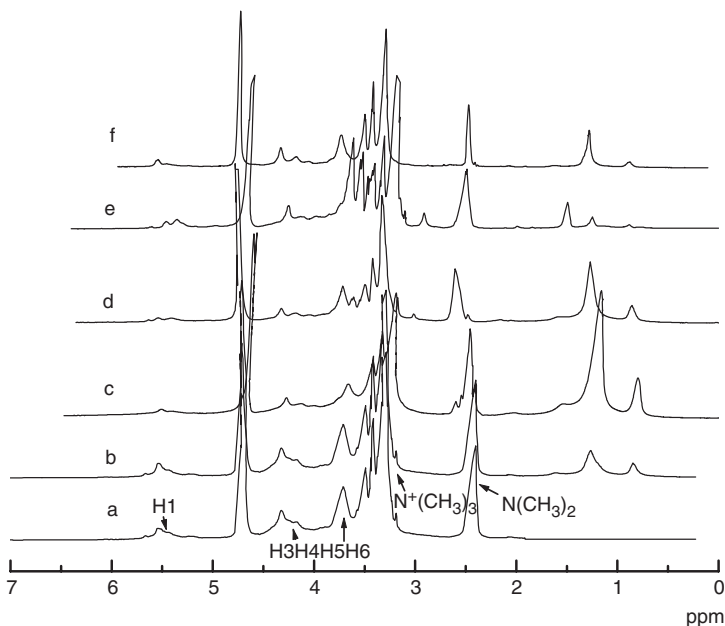


Figure 1. $^1\text{H-NMR}$ spectra of (a) 29 kDa TMC2, (b) 29 kDa TMC2DG, (c) 29 kDa TMC2LG, (d) 29 kDa TMC2MG, (e) 29 kDa TMC2PG, (f) 29 kDa TMC2SG (D_2O).

appeared in the $^1\text{H-NMR}$ spectra among 29,000 TMC2DG, 29,000 TMC2LG, 29,000 TMC2MG, 29,000 TMC2PG, and 29,000 TMC2SG, this was explained by the different substitute degree in each compound. Further evidence supporting the efficient coupling reaction was obtained from the $^{13}\text{C-NMR}$. Unlike 70,000 TMC1 and the 70,000 TMC2, 70,000 TMC1MG, and 70,000 TMC2MG show a $^{13}\text{C-NMR}$ signal at δ (ppm) 16.4 that was assigned to the methyl carbon ($-\text{OC}-(\text{CH}_2)_n-\underline{\text{C}}\text{H}_3$) of the long-chain acyl group and the signals at δ (ppm) 27.3, 38.1, and 39.7 were assigned to the methene carbons ($-\text{OC}-(\underline{\text{C}}\text{H}_2)_n-\text{CH}_3$) of the acyl long-chain. The chemical shifts observed for 162.7 and 164.7 were attributed to either the acid amide carbon ($-\text{NH}-\underline{\text{C}}\text{O}-$) or the ester ($-\text{O}-\underline{\text{C}}\text{O}-$) from long-chain acid chloride linking the $-\text{NH}_2$ or $-\text{OH}$ of 70,000 TMC1 and 70,000 TMC2, respectively.

To determine whether some of the $^1\text{H-NMR}$ spectra and $^{13}\text{C-NMR}$ peaks were not due to some free acyl chlorides (or corresponding carboxylates) of the long-chain saturated fatty acids not fully removed, the samples were characterized with FTIR. No absorption peak for the carboxylic acid carboxyl group (1700 cm^{-1}) was found in the IR spectra, indicating that no free long-chain carboxylic acid remained. The IR spectra of 70,000 TMC2DG, 70,000 TMC2LG, 70,000 TMC2MG, 70,000 TMC2PG, and 70,000 TMC2SG displayed intensive peaks at 2925, 2845, 1475, and 1383 cm^{-1} which were ascribed to $-\text{CH}_3$ and $-\text{CH}_2$ of long-chain acyl groups of the long-chain saturated fatty acyl grafting on the amine and hydroxyl groups of TMC. Moreover, Some prominent bands at 1640 and 1550 cm^{-1} were observed and assigned to the carbonyl stretching of amide I band and amide II band, respectively. As DS increased, the intensity of the carbonyl stretching of amide I and amide II increased; these data support *N*-acylation. The absorption peak at $\sim 1730\text{ cm}^{-1}$ was also observed in other IR spectra, which was estimated to be due to *O*-acyl esters [20].

All of the polymers synthesized by the coupling reaction between the long-chain saturated fatty acyl chloride and TMC were fully confirmed by $^1\text{H-NMR}$, $^{13}\text{C-NMR}$, and IR. The degree of substitution of long-chain acyl group of ATMC was calculated by $^1\text{H-NMR}$ using the ratio of the integral of the chemical shift of long-chain acyl group protons (δ 0.8–1.85 ppm) to the integral of ^1H protons peaks (δ 4.7–5.7 ppm) of chitosan (Table 1).

Critical Micelle Concentration

The CMC was obtained by pyrene excitation spectra. Only small, even negligible, fluctuations appear in total fluorescence intensity at 334 nm at low levels of 70,000 TMC2MG ($C < \text{CMC}$); however, as the

Table 1. DS of quaternary amino group (DS1) and long-chain acyl group (DS2) in chitosan derivatives, CyA concentration, LC, EE, particle size and polydispersity of chitosan derivative micelles ($n = 3$).

Sample	DS1 (%)	DS2 (%)	CyA concentration (mg/mL)	LC (%)	EE (%)	Particle size (nm)	Polydispersity
29,000 TMC2DG	45.2	8.8	0.32	12.5	49.1	257.9	0.08
29,000 TMC2LG	45.2	8.2	0.40	16.6	61.1	249.3	0.02
29,000 TMC2MG	45.2	7.6	0.39	16.9	60.8	312.2	0.43
29,000 TMC2PG	45.2	8.9	0.26	12.0	40.2	356.2	0.30
29,000 TMC2SG	45.2	8.1	0.32	9.6	48.6	259.4	0.07
70,000 TMC1DG	21.3	8.4	0.31	11.1	47.5	301.8	0.05
70,000 TMC1LG	21.3	8.2	0.32	12.7	49.4	324.1	0.13
70,000 TMC1MG	21.3	7.2	0.33	14.5	50.3	341.4	0.09
70,000 TMC1PG	21.3	7.8	0.32	11.7	49.9	295.4	0.04
70,000 TMC1SG	21.3	8.6	0.23	10.6	35.8	271.1	0.02
70,000 TMC2DG	44.8	8.2	0.32	11.5	48.6	246.0	0.11
70,000 TMC2LG	44.8	7.5	0.43	16.0	65.9	260.7	0.01
70,000 TMC2MG	44.8	8.2	0.41	17.1	63.3	347.3	0.09
70,000 TMC2PG	44.8	8.6	0.45	16.0	69.8	247.8	0.11
70,000 TMC2SG	44.8	7.7	0.28	12.3	43.4	250.6	0.03

concentration of the polymeric amphiphile increased, the excitation intensity rose as well. At CMC a remarkable increase in the total fluorescence intensity and a red shift of the band from 334 to 338 nm was observed (Figure 2) due to the transfer of the pyrene molecules from an aqueous environment to the hydrophobic micelle cores. Shown in Figure 2 is the intensity ratio (I338/I334) of the pyrene excitation spectra versus the logarithm of the 70,000 TMC2MG concentrations. Based on the intensity ratio data, the CMC values of 70,000 ATMC2s were calculated to be from 0.028 to 0.038 mg/mL (Table 2).

The relationship of CMC to the structure of the 70,000 ATMC2s was examined. Three structure parameters, DS of quaternary amino group, long-chain acyl groups, and chitosan unit by mole per kilogram, were introduced. The different degrees of substitution, DS, (mol/kg) was calculated by the following equations:

DS of quaternary amino group (mol/kg)

$$=1000 \cdot (\text{DS of quaternary amino group}) / \text{MW}_{(70\text{kATMC2s unit})} \quad (3)$$

DS of long chain acyl amino group (mol/kg)

$$=1000 \cdot (\text{DS of long - chain acyl group}) / \text{MW}_{(70\text{kATMC2s unit})} \quad (4)$$

DS of chitosan unit (mol/kg)

$$=1000 / \text{MW}_{(70\text{kATMC2s unit})} \quad (5)$$

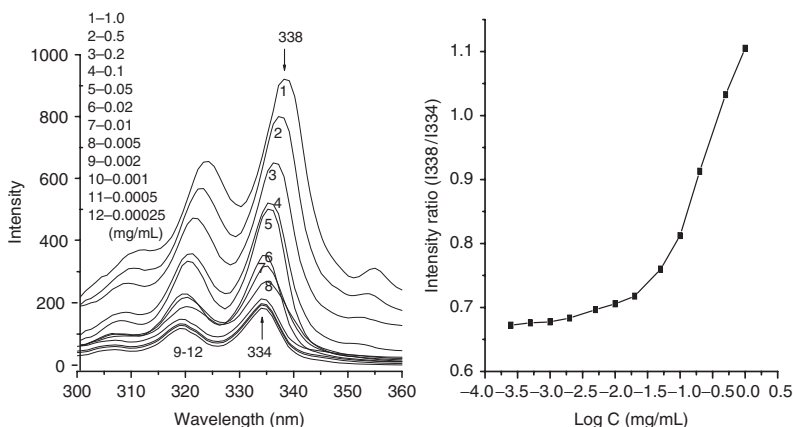


Figure 2. Pyrene excitation spectra (the final concentration of pyrene: 6×10^{-7} M) of 70 kDa TMC2MG in aqueous solutions ($\lambda_{em} = 390$ nm) and Intensity ratio plots of I338/I334 vs log C for 70 kDa TMC2MG in water.

Table 2. The DS of quaternary amino group (DS1), long-chain acyl groups (DS2) and chitosan unit (DS3), log CMC, and CMC of 70,000 ATMC2s.

Sample	DS 1 (mol/kg)	DS 2 (mol/kg)	DS 3 (mol/kg)	Log CMC	CMC (mg/mL)
70,000 TMC2DG	2.23	0.41	4.98	-1.42	0.038
70,000 TMC2LG	2.22	0.37	4.95	-1.45	0.035
70,000 TMC2MG	2.18	0.40	4.87	-1.54	0.029
70,000 TMC2PG	2.15	0.41	4.79	-1.52	0.030
70,000 TMC2SG	2.15	0.37	4.79	-1.55	0.028

where $MW_{(70,000ATMC2s \text{ unit})}$ represented the molar weight of the 70,000 ATMC2s unit [22]. The obtained values of these three structural parameters are listed in Table 2.

The absolute correlation coefficient (r) from the linear regression curves of log CMC vs DS of quaternary amino group (mol/kg) was greater than 0.9, which indicated a linear relative. But the correlation coefficient (r) of log CMC versus DS of long-chain acyl groups and chitosan unit (mol/kg) were within 0.9, due to the introduction of acyl groups of different carbon chain length into 70,000 TMC2.

Preparation and Characterization of Polymeric Cyclosporine A Micelles

Listed in Table 1 are the LC, EE, particle size and polydispersity of the CyA-loaded micelles. The LC and EC of ATMC micelles were 9.6–17.1%

and 35.8–69.8%, respectively, and the solubility of CyA in ATMC micellar solution was greatly improved. The highest concentration of CyA in the micellar solution was 0.45 mg/mL, and the micellar particle size ranged from 246.0 to 356.2 nm. A similar LC trend for all the three series of chitosan derivatives is seen in Figure 3. As the carbon chain length of acyl groups increased, the LC increased and reached a maximal point before the value went down. The same tendency was also observed for the EE and particle size values (Figure 3).

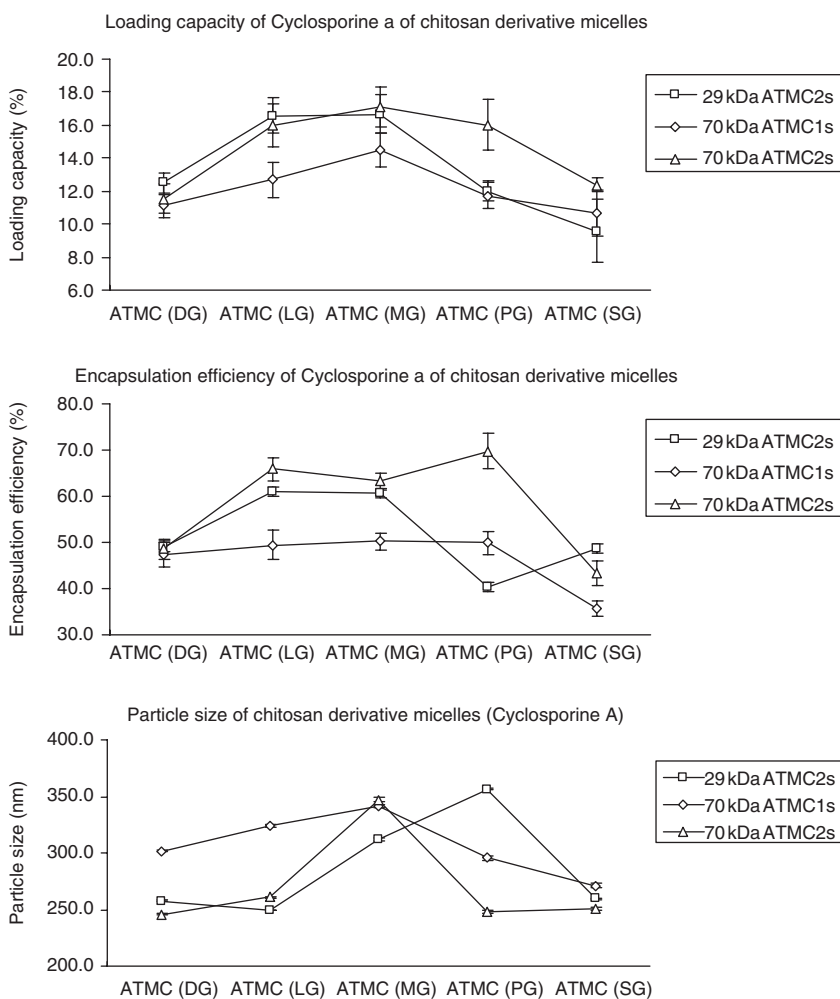


Figure 3. Loading capacity, EE and particle size of CyA-loaded micelles of chitosan derivative.

The connection between the LC and EC of micelles and the structural properties of the polymers that self-assembly form them was also investigated. The TEM micrograph of the ATMC micelles is presented in Figure 4, showing that ATMC was able to form nanoscale near-spherical micelles with slight deformation and aggregation. It was assumed that some structural properties of chitosan derivatives such as the methylation degree, long-chain acyl groups and molecular weight could play a role affecting the drug-loading capacity of the micelles. Thus an analysis of the variance of a single factor in every 2 series of chitosan derivatives was attempted.

A comparison of 70,000 ATMC1s and 70,000 ATMC2s indicated that greater CyA loading was attributable to a higher methylation degree. Although having a similar methylation degree, the 70,000 ATMC2s had better CyA loading ability than 29,000 ATMC2s; this may be a result of a greater molecule weight. Moreover, in each series of chitosan derivatives, the ATMC with myristyl acyl (C_{14}) had a maximal LC of drug. It seems that the acyl chain length that forms the core of solubilized micelles, in which the drug molecules can be incorporated, influences the entropically driven hydrophobic interactions. On the one hand, the shorter the chain of the saturated acyl group is, the more compact the micellar core is and hence the less efficient at solubilization. Although the longer hydrophobic segments enhanced the solubilization by increasing the partition coefficient, the solubilization capacity was lowered [1]. Consequently, the medium-sized long-chain acyl group (C_{14}) used in our study displayed the best CyA incorporation because the hydrophobic core provided a more suitable microenvironment for this hydrophobic agent.

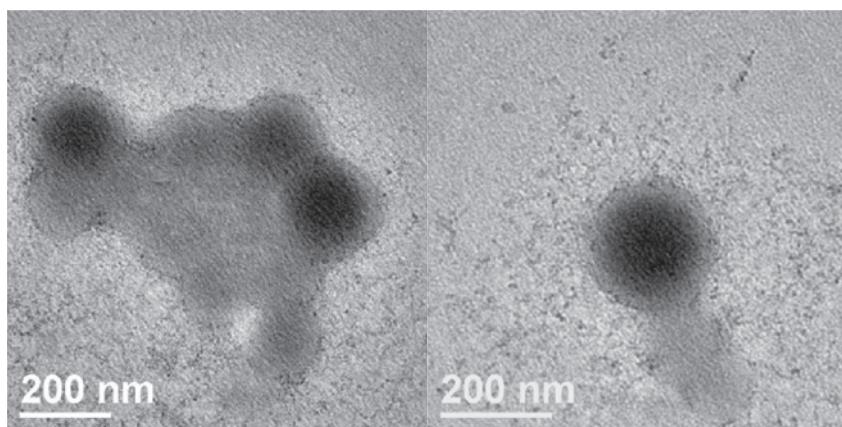


Figure 4. Transmission electron micrograph of CyA-loaded in ATMC micelles.

CONCLUSIONS

In summary, novel chitosan derivatives, *N*-acyl, *O*-acyl-*N*-trimethyl chitosan chloride (ATMC), were synthesized and confirmed by ¹H-NMR, ¹³C-NMR and FT-IR spectra, respectively. The amphiphilic ATMC would self-assemble to form micelles in the aqueous solution and had good solubilization ability of CyA. In our experiment, chitosan derivatives of high methylation degree, medium-sized long-chain acyl group (C₁₄), and large molecular weight had the best effect in loading CyA. So the ATMC micelle may be a promising carrier for poorly soluble drugs in drug delivery system.

ACKNOWLEDGMENT

This study is financially supported by National Natural Science Foundation of China (30772662), Program for New Century Excellent Talents in University (NCET-06-0499), Ministry of Education key project (107062), grant from the Ph.D. Programs Foundation (20070316004) and 111 Project from the Ministry of Education of China and the State Administration of Foreign Expert Affairs of China (No. 111-2-07).

REFERENCES

1. Bromberg, L. (2008). Polymeric Micelles in Oral Chemotherapy, *Journal of Controlled Release*, doi:10.1016/j.jconrel.2008.01.018.
2. Lu, H.W., Zhang, L.M., Liu, J.Y. and Chen, R.F. (2008). Synthesis of an Amphiphilic Polysaccharide Derivative and its Micellization for Drug Release, *Journal of Bioactive and Compatible Polymers*, **23**: 154–170.
3. Li, Q., Dunn, E.T., Grandmaison, E.W. and Goosen, M.F.A. (1992). Applications and Properties of Chitosan, *Journal of Bioactive and Compatible Polymers*, **7**: 370–397.
4. Wang, X.H., Cui, F.Z., Feng, Q.L., Li, J.C. and Zhang, Y.H. (2003). Preparation and Characterization of Collagen/Chitosan Matrices as Potential Biomaterials, *Journal of Bioactive and Compatible Polymers*, **18**: 453–467.
5. Ravi Kumar, M.N.V. (2000). A Review of Chitin and Chitosan Applications, *Reactive and Functional Polymers*, **46**(1): 1–27.
6. Tien, C.L., Lacroix, M., Ispas-Szabo, P. and Mateescu, M.-A. (2003). *N*-acylated Chitosan: Hydrophobic Matrices for Controlled Drug Release, *Journal of Controlled Release*, **93**: 1–13.
7. Avadi, M.R., Erfan, M., Sadeghi, A.M.M., Moezi, L., Dehpour, A.R., Younessi, P., Rafiee Tehrani, M. and Shafiee, A. (2004). *N*, *N*-Diethyl-*N*-Methyl Chitosan as an Enhancing Agent for Colon Drug Delivery, *Journal of Bioactive and Compatible Polymers*, **19**: 421–433.

8. Bayat, A., Sadeghi, A.M.M., Avadi, M.R., Amini, M., Rafiee-Tehrani, M., Shafiee, A. et al. (2006). Synthesis of *N,N*-dimethyl *N*-ethyl Chitosan as a Carrier for Oral Delivery of Peptide Drugs, *Journal of Bioactive and Compatible Polymers*, **21**: 433–444.
9. Sadeghi, A., Avadi, M., Siedi, F., Rafiee-Tehrani, M. and Ginger, H.E. (2008) Synthesis, Characterization and Antibacterial Effects of Trimethylated and Triethylated 6-NH₂-6-deoxy Chitosan, *Journal of Bioactive and Compatible Polymers*, **23**: 223–234.
10. Bejugam, N.K., Sou, M., Uddin, A.N., Gayakwad, S.G. and D'Souza, M.J. (2008). Effect of Chitosans and Other Excipients on the Permeation of Ketotifen, FITC-Dextran, and Rhodamine 123 through Caco-2 Cells, *Journal of Bioactive and Compatible Polymers*, **23**: 187–202.
11. Bernkop-Schnürch, A. (2000). Chitosan and its Derivatives: Potential Excipients for Peroral Peptide Delivery Systems, *International Journal of Pharmaceutics*, **194**: 1–13.
12. Denkbass, E.B. and Ottenbrite, R.M. (2006). Perspectives on: Chitosan Drug Delivery Systems Based on their Geometries, *Journal of Bioactive and Compatible Polymers*, **21**: 351–368.
13. Kotze', A.F., Lueßen, H.L., De Leeuw, B.J., De Boer, A.G., Verhoef, J.C. and Junginger, H.E. (1997). *N*-trimethylchitosan Chloride as a Potential Absorption Enhancer Across Mucosal Surfaces: *In vitro* Evaluation in Intestinal Epithelial Cells (Caco-2), *Pharmaceutical Research*, **14**(9): 1197–1202.
14. Thanou, M., Florea, B.I., Langemeyer, M.W.E., Verhoef, J.C. and Junginger, H.E. (2000). *N*-trimethylchitosan Chloride (TMC) Improves the Intestinal Permeation of the Peptide Drug Buserelin in vitro (Caco-2 cells) and in vivo (rats), *Pharmaceutical Research*, **17**(1): 27–31.
15. Zhang, C., Ping, Q.N., Zhang, H.J. and Shen, J. (2003). Preparation of *N*-alkyl-*O*-sulfate Chitosan Derivatives and Micellar Solubilization of Taxol, *Carbohydrate Polymers*, **54**(2): 137–141.
16. Zhang, C., Qu, G.W., Sun, Y.J., Wu, X.L., Yao, Z., Guo, Q.L. et al. (2008). Pharmacokinetics, Biodistribution, Efficacy and Safety of *N*-octyl-*O*-sulfate Chitosan Micelles Loaded with Paclitaxel, *Biomaterials*, **29**(9): 1233–1241.
17. Aungst, B.J., Saitoh, H., Burcham, D.L., Huang, S.-M., Mousa, S.A. and Hussain, M.A. (1996) Enhancement of the Intestinal Absorption of Peptides and Non-peptides, *Journal of Controlled Release*, **41**(1–2): 19–31.
18. Dattatraya, S.S.S.S., Rao, C.K. and Govind, K.S. Indian Patent, NO.187,162A (1998).
19. Vasnev, V.A., Tarasov, A.I., Markova, G.D., Vinogradova, S.V. and Garkusha, O.G. (2006). Synthesis and Properties of Acylated Chitin and Chitosan Derivatives, *Carbohydrate Polymers*, **64**(2): 184–189.
20. Tong, Y.J., Wang, S.F., Xu, J.W., Chua, B.S. and He, C.B. (2005). Synthesis of *O,O'*-dipalmitoyl Chitosan and Its Amphiphilic Properties and Capability of Cholesterol Absorption, *Carbohydrate Polymers*, **60**(2): 229–233.

21. Astafieva, I., Zhong, X.F. and Eisenberg', A. (1993). Critical Micellization Phenomena in Block Polyelectrolyte Solutions, *Macromolecules*, **26**(26): 7339–7352.
22. Yao, Z., Zhang, C., Ping, Q.N. and Yu, L.L. (2007). A Series of Novel Chitosan Derivatives: Synthesis, Characterization and Micellar Solubilization of Paclitaxel, *Carbohydrate Polymers*, **68**(4): 781–792.
23. Zhang, C., Ding, Y., Yu, L.L. and Ping, Q.N. (2007). Polymeric Micelle Systems of Hydroxycamptothecin Based on Amphiphilic *N*-alkyl-*N*-trimethyl Chitosan Derivatives, *Colloids and Surfaces B: Biointerfaces*, **55**(2): 192–199.
24. Ugazio, E., Cavalli, R. and Gasco, M.R. (2002). Incorporation of Cyclosporin A in Solid Lipid Nanoparticles (SLN), *International Journal of Pharmaceutics*, **241**(2): 341–344.
25. Zong, Z., Kimura, Y., Takahashi, M. and Yamane, H. (2000). Characterization of Chemical and Solid State Structures of Acylated Chitosans, *Polymer*, **41**(3): 899–906.
26. Snyman, D., Hamman, J.H., Kotze, J.S., Rollings, J.E. and Kotze', A.F. (2002). The Relationship between the Absolute Molecular Weight and the Degree of Quaternisation of *N*-trimethyl Chitosan Chloride, *Carbohydrate Polymers*, **50**(2): 145–150.